REVISTA SOLDAGEM & INSPEÇÃO

ISSN 1980-6973 (Online) | ISSN 0104-9224 (Print)

ORIGINAL PAPER

Prediction of Microstructural and Mechanical Properties of Steel Welds with Artificial Neural Networks

Sabrican Demir[1], **Mustafa Şahin**[2], **Şükrü Talaş**[3]

[1] Afyon Kocatepe University, Institute of Natural Sciences, Afyonkarahisar, Türkiye.

[2] University of Health Sciences, Department of Electronics and Automation, Istanbul, Türkiye.

[3] Afyon Kocatepe University, Faculty of Technology, Department of Metallurgical and Materials Engineering, Afyonkarahisar, Türkiye.

How to cite: Demir S, Şahin M, Talaş S. Prediction of microstructural and mechanical properties of steel welds with artificial neural networks. Rev. Soldag. Insp. 2025;30:e3007. https://doi.org/10.1590/0104-9224/SI30.07

Abstract: The mechanical properties of the weld metals are dependent on the alloying elements and the microstructure of the weld metal. Neural network analysis is widely applicable in various fields, aiming to enhance efficiency thorough analysis. The application of artificial intelligence techniques for the rapid and accurate determination of physical properties offers a significant time, cost and labor advantage in industrial production processes due to the time consuming and costly nature of traditional methods. This study was aimed to investigate the relationships between structural and microstructural properties against alloying elements in SMAW weld metal using neural networks and to analyze them through this innovative methodology. In this study, the Levenberg-Marquardt algorithm is utilized to predict the physical properties of weld metal through artificial neural networks approach using 94 sets of weld metal composition and microstructural properties. The success rates of the modelling were found to be 93.14% for acicular ferrite, 95.92% for hardness, 94.17% for yield strength, and 96.32% for ultimate tensile strength. It is also feasible to make reverse predictions of weld metal composition in order to predict weld metal properties such as hardness, yield strength, acicular ferrite percentage and ultimate tensile strength within a range of alloying elements percentages, with a reasonable degree of accuracy.

Key-words: Artificial neural networks; Weld metal; Acicular ferrite; Mechanical properties.

1. Introduction

In the field of materials science, the application of machine learning, particularly neural networks inspired by the human brain, has gained significant traction in recent years. One of the key challenges in materials development is understanding how desired properties, such as yield strength, toughness, ultimate tensile strength, and fatigue life, are affected by factors like intrinsic microstructure, chemical composition, crystal structure, and external processing, loading conditions, and temperatures. Machine learning algorithms are capable of establishing quantitative relationships between independent variables (like composition and processing conditions) and dependent variables (such as mechanical properties), facilitating accurate predictions in scenarios where physical models are either unavailable or overly complex.

Neural networks have demonstrated their ability to handle complex models, making them a suitable choice for predicting the properties of materials, such as the toughness of ferritic steel welds [1-3]. The use of neural networks in materials science has been explored for various applications, including phase selection in multi-principal element alloys [1] and the prediction of mechanical properties [4]. In the context of weld metal composition prediction, neural networks can be a valuable tool, as the relationship between the chemical composition of the weld metal and its properties can be highly complex and non-linear. Fortunately, recent advances in artificial intelligence have made it possible to reduce costs, labour and time in many areas. The use of artificial intelligence is becoming increasingly widespread, particularly in solving complex and data-driven problems [5-8]. Conventional approaches to evaluating these characteristics are often lengthy and very costly. Consequently, leveraging artificial intelligence techniques to predict these properties expeditiously and accurately provides significant advantages in terms of cost and time reduction. The architecture of artificial neural networks comprises interconnected neurons organized in layers. The input layer receives inputs, which are subsequently processed by the network to generate outputs in the final layer. This process of determining parameter coefficients is facilitated by a learning process. The structure of artificial neural networks includes at least an input layer, an output layer and one or more hidden layers between these layers. Each layer contains one or more groups of neurons. The connections between layers are determined by weights/coefficients that are

Received: 13 Nov., 2024. Accepted: 07 Apr., 2025.
E-mails: sabricandemir@yahoo.com (SD), mustafa.sahin4@sbu.edu.tr (MS), stalas@aku.edu.tr (ST)

established during the learning process of the network. These weights influence the behaviour of the network, allowing inputs to be transmitted, operations to be performed and outputs to be produced [9].

One of the main applications of artificial intelligence is in manufacturing, such as welding of similar and dissimilar metals. The properties of the weld metal are directly related to the alloy content of the base metal and filler metal used. However, the properties of the weld metal are also influenced by the thickness of the base material, the welding current, the welding time and the size of the base material. These parameters can cause calculation difficulties when investigating the properties of the weld metal. Therefore, in order to analyse the mechanical and physical properties of the weld metal, it is useful to study the effect of composition as the main parameter while keeping other parameters constant. This can be done using a powerful analysis methodology such as artificial intelligence. The analysis should include commonly used compositional elements such as C, Mn, Si, Ti, etc. as well as yield strength (YS), ultimate tensile strength (UTS), hardness (HRD) and acicular ferrite (AF) percentage [10]. The elemental ratios in the weld metal have a direct influence on its physical properties and weldability and thus on the overall weld quality. The resistance spot welding of 2205 duplex steel was selected to estimate the weld core geometry [11]. The MATLAB 7.0 Neural Network Toolbox was used with the Back Propagation (BP) algorithm as the learning algorithm, resulting in a 97.63% successful prediction rate. Similar success rate was also obtained in a study [12] that used artificial intelligence to estimate the fatigue life of 73 steels. The fatigue strength coefficient was estimated to be 99% and the fatigue strain coefficient was estimated to be 98%. The potential of neural networks in estimating the quality of weld strength and dimensions in laser welding of thermoplastic sheets were carried out [13]. The results suggest that neural networks can serve as an alternative method in improving the parametric systems. A genetic algorithm was used to determine the near-optimal process parameters for friction welding [14]. The input data for this study included tool speed, tool profile and tool feed rate, while the output parameters were tensile strength, yield strength, elongation and hardness. The properties of the weld core were estimated after laser welding of 6 mm thick aluminium alloy plates [15]. Taguchi method was successfully used to predict the weld width in submerged arc welding [16]. A statistical analysis of tensile test results using artificial neural networks and Taguchi approaches for welding parameters of stainless steels were studied [17] and the artificial neural network produced highly reliable results, with successful agreement with experimental results and low error rates. The UTS of the welded joints was predicted using both artificial neural network and Taguchi methods with an accuracy of 96.97% and 78.31%, respectively. The artificial neural network was used to assess the quality of welds in the gas metal arc welding process [18]. In the training process, the overall classification accuracy was found to be 94.7%. The quality of the test welds was accurately predicted by the artificial neural network they used with an accuracy of 90.9%.

The objective of this study is to utilize the Levenberg-Marquardt (LM) algorithm to train an artificial neural network to predict the physical properties of weld metal and vice versa. The effectiveness of this method is compared with other prediction methods to determine the most appropriate method. The relationship between weld composition and weld metal properties is analysed as a basis for this study.

2. Materials and Method

2.1. Input data and related process

Acicular ferrite (AF) has been identified as a particularly advantageous microstructure in the case of low alloy steel weld metals, due to the fact that it provides enhanced values for both optimum toughness and yield strength, as well as ultimate tensile strength (UTS), when contrasted with other structures, namely grain boundary ferrite or ferrite side plate structures. For this reason, this particular microstructure is a primary focus in the present study. From the works of G.M. Evans [19-29], a data set containing 94 sets of weld metal compositions and their mechanical properties and AF percentages (statistical analysis of data is presented in Table 1) has been compiled containing the percentages of the elements C, Si, Mn, Al, Ti, Nb, V, Mo, Cr, Ni, Cu and N in the weld metal of Shielded Metal Arc Welding (SMAW, rutile electrode, all other parameters were kept the same). The present study investigates the relationship between the variation in the proportions of the chemical elements C, Si, N, Mn, Al, Ti, Nb, V, Mo, Cr, Ni and Cu, in the weld metal, and the mechanical properties as HRD, YS and UTS, and the microstructural property of the AF content. An artificial neural network analysis was employed to make predictions about the composition of the weld metal in order to establish correlations between the compositions and the mechanical and microstructural properties. The artificial neural network (ANN) network was trained with pre-obtained data, and predictions were made with the trained weld metal compositions and properties. The collected data set was processed using MATLAB software. The experimental data were normalised and subjected to the necessary transformations to better understand the relationship between the properties.

Table 1. The statistical properties of weld metal properties and their compositions used in this study (in wt%).

	Median	Standard Deviation	Minimum	Maximum	Average
C	0.0685	0.0208	0.0147	0.1480	0.0636
Si	0.3300	0.1068	0.2000	0.9500	0.3550
Mn	1.3500	0.3919	0.6000	1.8500	1.2313
Al	0.0005	0.0088	0.0005	0.0610	0.0023
Ti	0.0035	0.0032	0.0006	0.0255	0.0042
Nb	0.0005	0.0148	0.0005	0.0940	0.0041
V	0.0005	0.0168	0.0003	0.1000	0.0050
Mo	0.0005	0.1285	0.0005	1.1100	0.0207
Cr	0.0005	0.3801	0.0005	2.3800	0.0901
Ni	0.0005	0.6158	0.0005	3.4600	0.1574
Cu	0.0005	0.1635	0.0005	1.4000	0.0295
N	0.0070	0.0014	0.0010	0.0110	0.0071
AF (%)	62	23.5370	0	89	62
HRD (HV)	214.5	26.8011	160	324	214.5
YS (MPa)	490	70.5664	391	808	490
UTS (MPa)	559	66.6984	453	865	559

2.2. ANN processing of weld metal composition data

The architecture of artificial neural networks comprises processing elements, including input, weights, transfer function, activation functions, and output. The input elements, which are data utilized for processing, can be of various types, including numerical or categorical values. The dimensions and format of these input elements depend on the intended application of the network and the nature of the data [30]. Inputs are important in the learning process of the network and this learning process trains the network to recognise patterns in the data and use them for classification, prediction or other tasks. Artificial neural networks use various mathematical operations to process the inputs, which reveal the relationships between the inputs and extract their attributes to produce the output of the network [31]. The size of the inputs, which refers to the number of features in the input data, is a critical aspect of network design. It plays a crucial role because different types of neural networks are specifically tailored to process inputs of varying sizes. A comprehensive understanding of this relationship is essential for optimizing network performance and ensuring effective data processing [32].

2.2.1. Normalisation process

In the process of preparing data for neural network training, it is possible to observe values in the data pool that are larger or smaller than expected. When such values are utilised during the training of the network, they have the potential to cause the network to incorrectly calculate the network inputs. To avoid this, it is important to normalise all data to be used in training to the range between 0 and 1. This normalisation process reduces the effect of the largest or smallest values in the data pool on the network. In order to enhance the efficacy of artificial neural network training, it is imperative to implement this normalisation process prior to starting the training phase of the ANN [33]. In this study, the data were normalised using the min-max normalisation technique. This technique involves the assignment of the lowest value in the dataset to the minimum and the highest value to the maximum. Equation 1 was utilised in order to reduce the data set to a range between zero and one. This ensured that the scales of the data were harmonised and the neural network was able to be trained correctly.

$$X' = \frac{X_i - X_{min}}{X_{max} - X_{min}} \quad (1)$$

where: X' = normalised value; X_i = Value to be normalised in the data pool; X_{max} = The largest entry in the data repository; X_{min} = Indicates the smallest entry in the data pool [34].

2.2.2. The formation of artificial neural network model

Artificial neural networks were used to model the relationship between the composition of the weld metal and microstructural properties. Input and output layers, hidden layers and appropriate activation functions were determined for the correct functioning of the model (Figure 1). In this study, a feed-forward back-propagation network structure was

preferred. The main reason for choosing this neural network structure is that the learning performance can be improved by the hidden layer. Table 2 summarises the parameters used in the creation of the ANN model used in the study and their relationship with output parameters, which are Acicular Ferrite (AF), Hardness (HRD), Yield Strength (YS) and Ultimate Tensile Strength (UTS). The output parameters are in total of 4, that are, AF, HRD, YS and UTS.

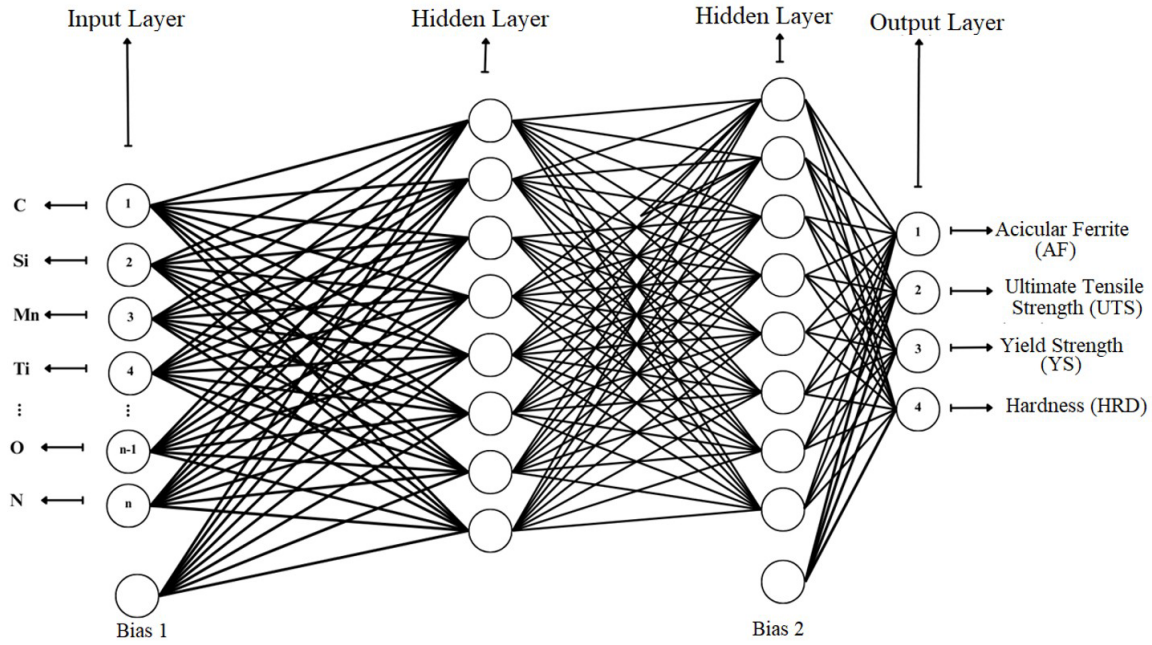

Figure 1. Schematic representation of ANN for this study.

Table 2. Parameters used in the formation of the ANN model.

Type of Network	Gradient based Network
Training Algorithm	TRAINLM
Trigger Function	TANSIG
Learning Function	LEARNGDM
Number of Neurons	20
Performance assesment Functions	MAPE

2.2.3. Training and testing of data

Neural Network Toolbox (NNT) in MATLAB software is a tool designed to use ANN without writing code. 94 input values were selected for the input data section and 4 target values were selected for the target data section. As seen in Figure 2, Feed-forward back-propagation was selected as the network type, Tansig activation as the activation function, and Levenberg-Marquardt (LM) algorithm [35-37] as the learning algorithm and other ANN models available in MATLAB Neural Network Toolbox were also studied, keeping the data and other parameters same for other algorithms. As given in Figure 3, the most efficient number of layers was found to be 13 in total and the number of neurons was found to be 20. The random search parameter was used based on our previous experience and the appropriate number of layers and neurons was reached after approximately 15 trials. Based on the experimental results, data set was trained until the error rate was minimised. The minimum error rate was achieved at the 6^{th} iteration for AF, HRD, YS and 9^{th} iteration for UTS, and the network was saved in MATLAB software.

The trained neural network model was used to predict the composition of 24 weld metal compositions and to model the behaviour of the desired weld metal based on the weld metal properties of AF, HRD, YS and UTS using the weld metal composition data used for the prediction.

The total number of data in the input parameters are 14 i.e. (**C** (16 variants), **Si** (8 variants), **Mn** (4 variants), **Ti** (10 variants), **Al** (6 variants), **Nb** (10 variants), **V** (10 variants), **Mo** (4 variants), **Cr** (10 variants), **Cu** (6 variants), **Ni** (10 variants))

with a total of 94 data entries. For the comparison of outputs MAPE classification was used [32]. The range of success rate based on MAPE performance classification is given in Table 3.

In this study, the performance parameters Absolute Percentage Error (MAPE), Correlation (R) and Coefficient of Determination (R^2) were used to evaluate the success of the created network. In estimation studies, it is desired for the MAPE value to be close to 0. Networks with a MAPE value below 10% are categorized as "very good", networks between 10% and 20% as "good", networks between 20% and 50% as "acceptable" and networks above 50% as "faulty/unsuccessful" networks [34]. In estimation studies, it is desired that the R^2 value is close to 1, which indicates that measured values and estimated values are close to each other.

Table 3. MAPE success performance percentage ranges [32].

MAPE	%10 and below	%10-%20	%20-%50	%50 and above
	Very good	Good	Pass	Unsuccessful

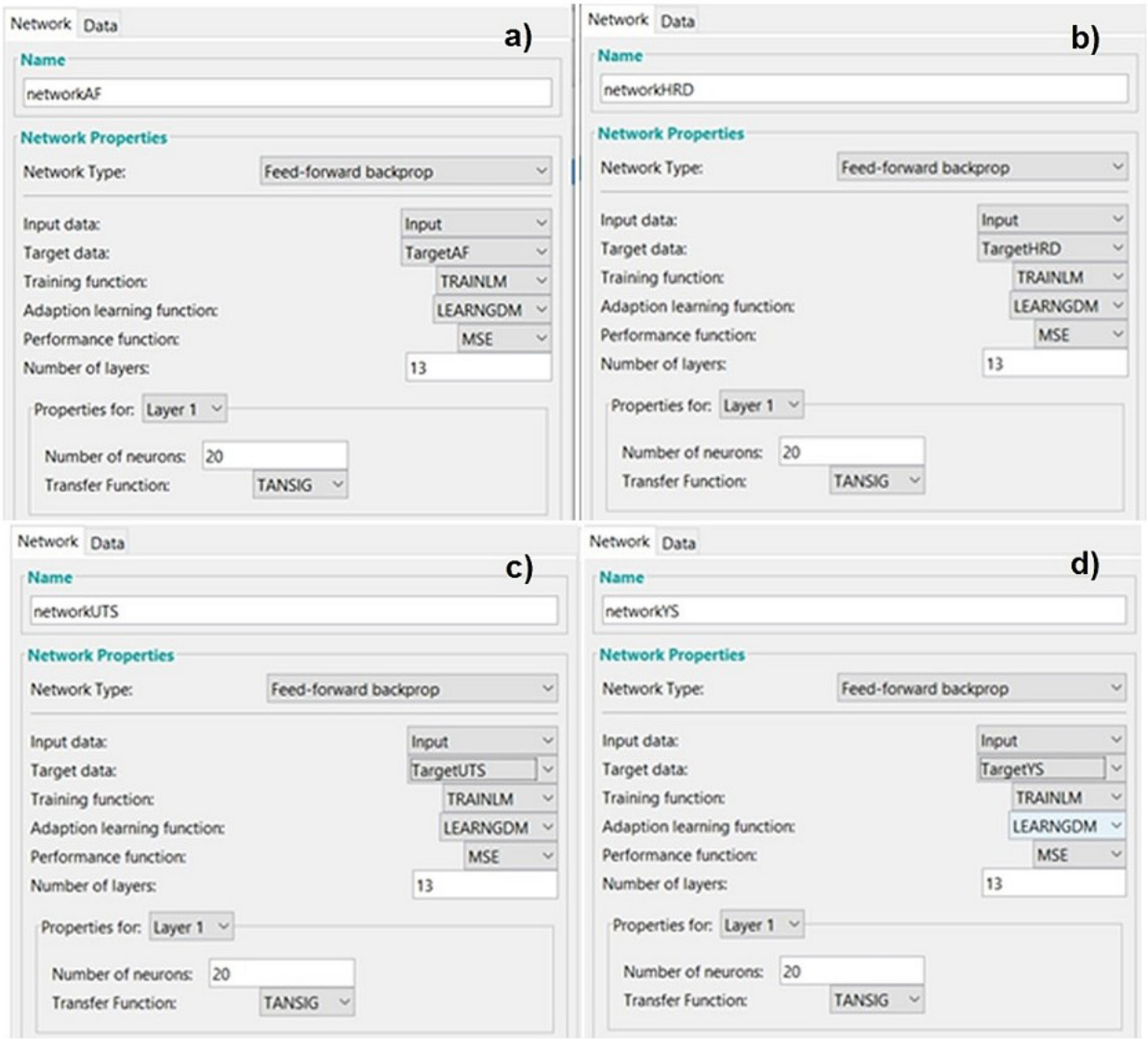

Figure 2. Network or data formation for (a) AF; (b) HRD; (c) UTS; (d) YS.

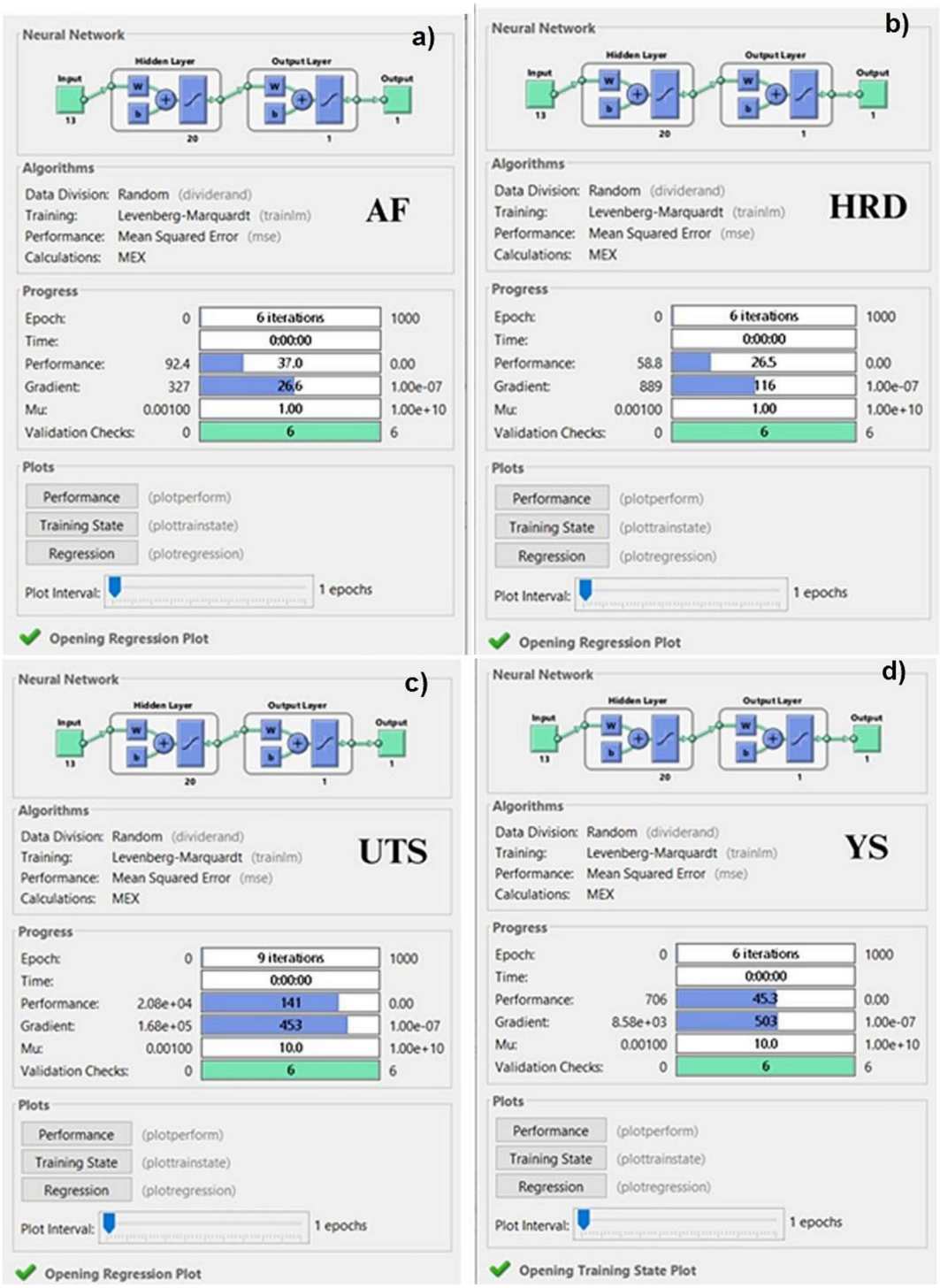

Figure 3. Training neural network settings using network tools for (a) AF; (b) HRD; (c) UTS; (d) YS.

3. Results and Discussion

3.1. Analysis of ANN training results

The Levenberg-Marquardt algorithm (LM) was utilised for the training of the network. Furthermore, the experiment was replicated with other artificial neural network (ANN) models, using the same data and parameters. The outcomes of these experiments were then compared to determine the repeatability of the results. As illustrated in Table 4, a comparison is made between the artificial neural network (ANN) models employed in the study and their respective overall success rates with respect to the approximation of real values. The learning function employed was LEARNGDM, while the activation function chosen was the Tangent-Sigmoid. The performance of the ANNs was evaluated using the mean absolute percentage error (MAPE) criterion.

Table 4. Comparison of Model Approximation Success Rates of Some Artificial Neural Networks.

	AF	HRD	YS	UTS
LM	93,135%	95,923%	94,17%	96,324%
SCG	73,917%	86,366%	93,64%	93,723%
BR	87,259%	96,837%	97,437%	99,200%
CGB	94,656%	93,558%	94,422%	92,661%
RP	75,263%	70,844%	95,935%	76,982%
BFG	99,623%	95,172%	99,671%	45.85%

LM: Levenberg-Marquardt; BR: Bayesian Regularisation; SCG: Scaled Conjugate Gradient; RP: Resilient Back propagation; BFG: BFGS Quasi Newton.

The optimal number of layers was determined to be 13 in total, with a total of 20 neurons The dataset was trained until the error rate was minimised, in accordance with the experimental results. The results of the analysis of the predictions obtained with the Levenberg-Marquardt algorithm (LM) and the actual data are provided in Table 5. The performance of the network was evaluated using the mean absolute percentage error (MAPE) method and R^2. A comparison of efficiency of fitting with the input data and modelling is made between the training data for Neural Network Training Regression, the test data, the validation data and the model approximation data for AF, HRD, YS and UTS input values against real values in Table 5. According to the MAPE classification, all results can be considered highly successful as shown in Table 5, however, overall results for AF appears to be lower than those of remaining HRD, YS and UTS results, which may be related to the one single non-fitting input (please see Figures 4-7).

Table 5. ANN training results for training data, validation data, test data and overall model output approximation rates against real values.

	Training Data	Validation Data	Test Data	Overall
AF	91.60%	96.04%	98.30%	93.14%
HRD	91.76%,	98.21%	98.79%	95.92%.
YS	95.44%	99.03%	97.29%	96.32%
UTS	92.27%,	99.09%	98.04%	94.17%

Please see Figures 4-7.

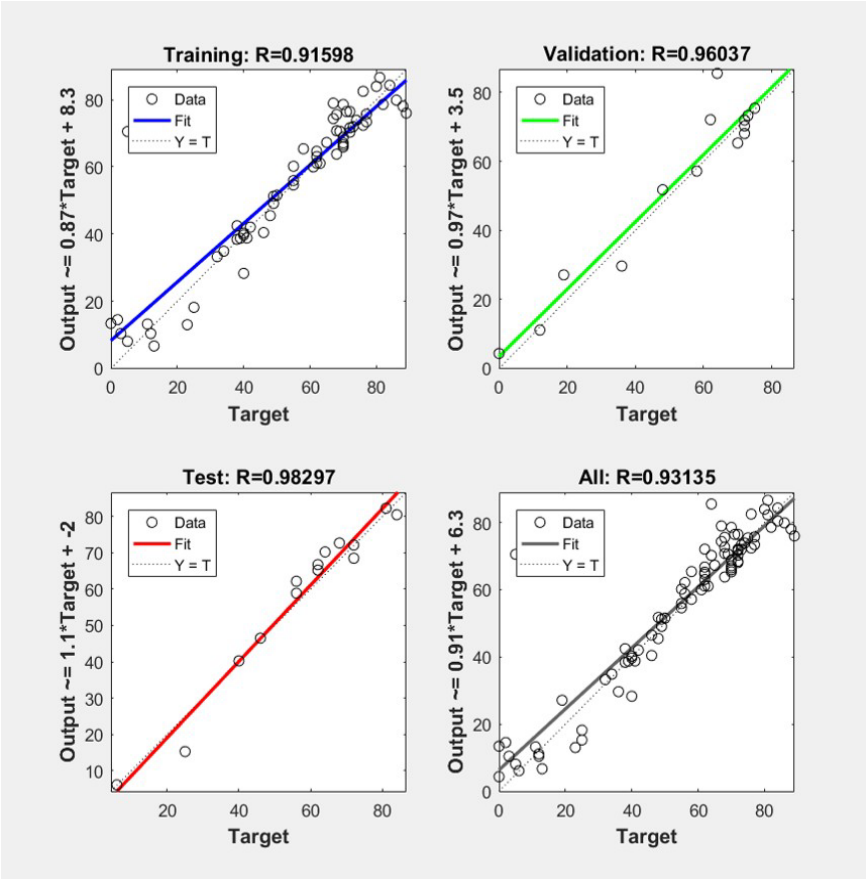

Figure 4. Neural Network Training Regression for Acicular Ferrite.

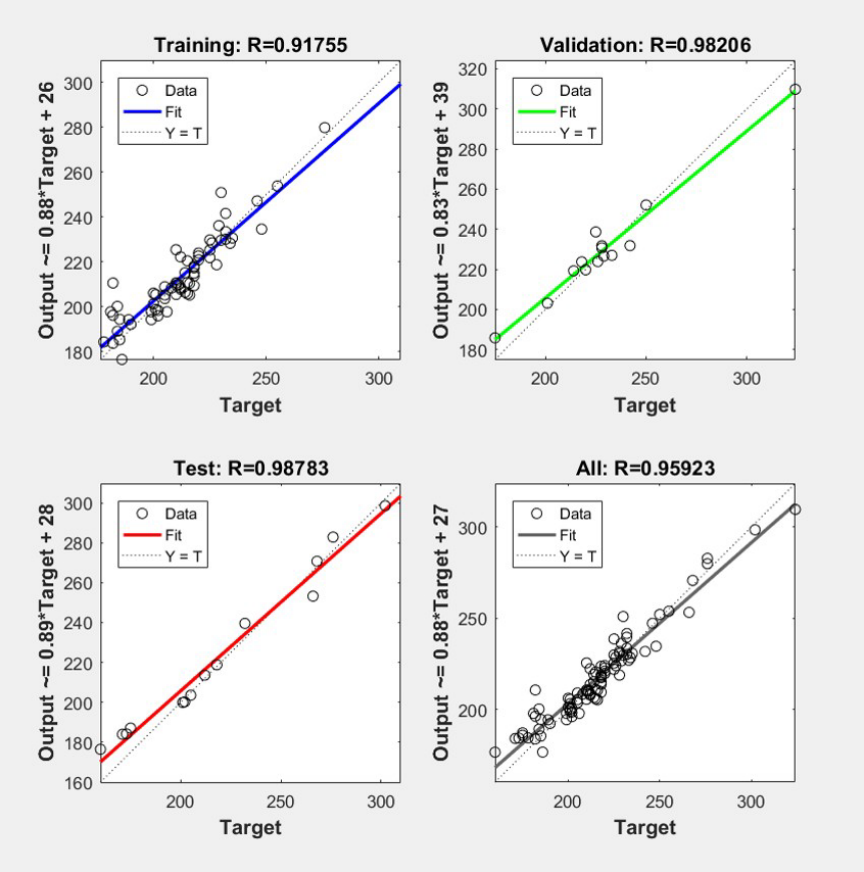

Figure 5. Neural Network Training Regression for hardness.

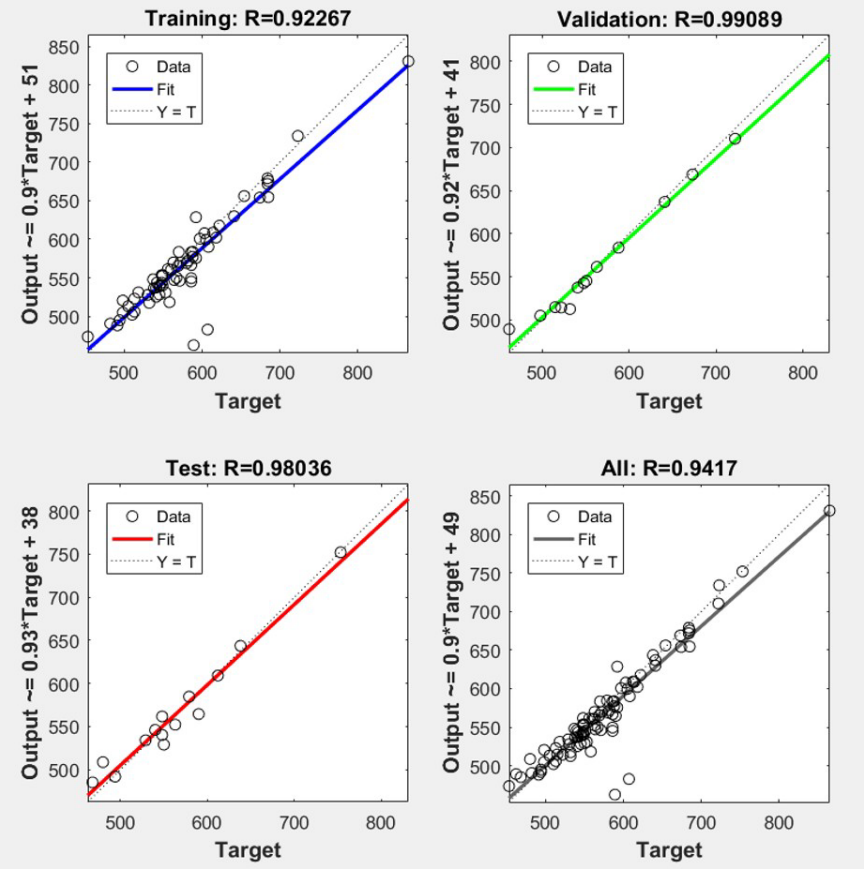

Figure 6. Neural Network Training Regression for Ultimate Tensile Strength.

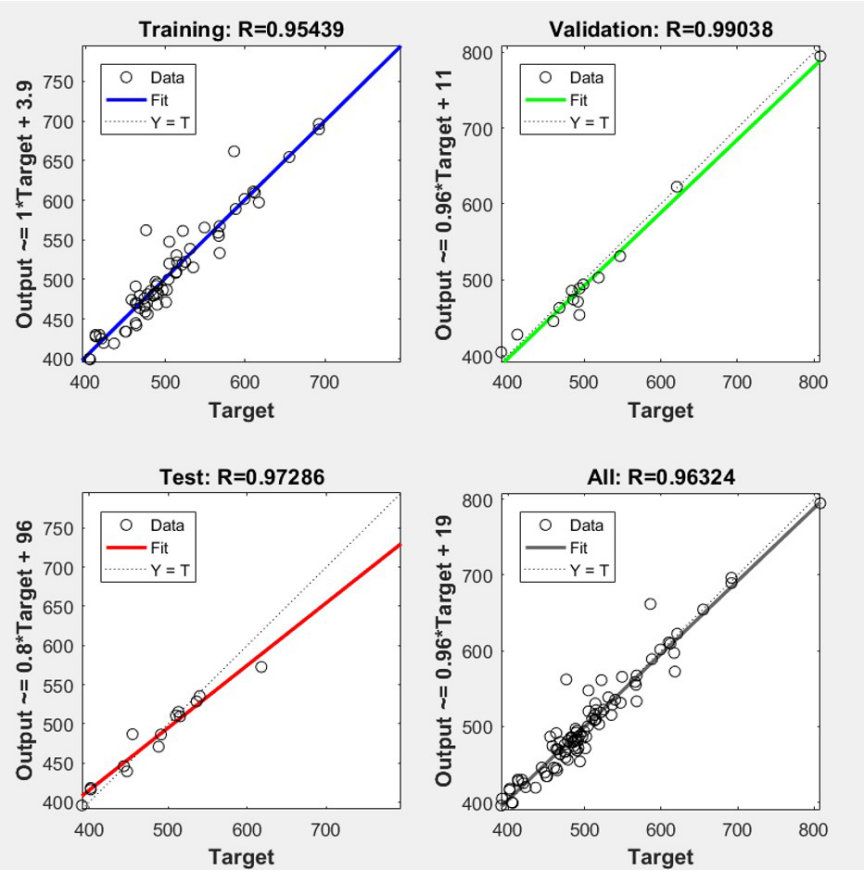

Figure 7. Neural Network Training Regression for Yield Strength.

The HRD, YS and UTS values are obtained by experimental means; that is to say, the results are measured by sensors and are less questionable. However, the percentage measurements of AF are carried out on micrographs and are more user-dependent. It is possible that these measurements may be influenced by the user's experience. This should be considered within the marginal error range and can be omitted as it is carried out according to standards [19-28].

3.2. Analysis of input data

The data used in this study can also be obtained from Demir [38]. For carbon and manganese, with increasing carbon content, there is a corresponding increase in hardness, yield strength, ultimate tensile strength and acicular ferrite percentage. Elevated carbon content make the arc more challenging to initiate and increases the weld metal brittleness in excess amount. The addition of manganese was increased with the objective of reducing these negative effects of carbon [39-43]. An increase in the silicon to manganese ratio resulted in enhanced hardness, the formation of acicular ferrite, elevated yield strength and ultimate tensile strength. The addition of Mn in increasing amount of C provides a decrease in disadvantages associated with elevated C levels [39,41,43]. This is achieved by enhancing the stability of the arc, optimising the shape of the plasma core, improving penetration and facilitating control during the welding process. Consequently, there was an increase in acicular ferrite, hardness, yield strength and ultimate tensile strength. It should be noted that the observed increase in mechanical properties is a consequence of the elevated carbon content in the weld metal [39,40]. The Ti percentage variation with respect to the amount of acicular ferrite, yield strength, and ultimate tensile strength exhibited a notable increase in all four parameters. The hardness of the weld metal exhibited a slight increase with elevated titanium content [39,44,45]. Ti reacts with elements such as oxygen and nitrogen present in the weld metal to form stable titanium nitrides or titanium carbonitrides. These reaction products affect the microstructure of the weld metal, thereby modifying its mechanical properties in general. Al on the other hand is considered not desired for the steel weld metals in high amounts and hence, the increase in Al percentage results in a reduction in the acicular ferrite ratio, accompanied by a slight increase in hardness, yield strength and ultimate tensile strength. The presence of aluminium in the weld pool serve to reduce the formation of pores by reacting with oxygen. This results in an improvement in the quality of the weld and an enhancement in the mechanical properties. The reduction in the acicular ferrite ratio can be attributed to the adverse effect of aluminium on the dissolution of intragranular microstructural features [39,40,46]. For Nb, Mn, given that an increase in Nb is associated with an elevated risk of cracking in the weld metal, the Mn and nitrogen ratios have been modified with the objective of enhancing the quality of the weld [39,47-49]. As the Nb ratio is increased, there was a corresponding

increase in HRD, YS and UTS values. The formation of acicular ferrite is not influenced by the presence of the Nb element but the percentage of acicular ferrite is subject to alteration by the exchange of nitrogen and oxygen. In data series, the percentages of V, Mn and Cr are provided with parametric variation. With decreasing percentage of vanadium content, there is an increase in acicular ferrite ratio, hardness, yield strength and ultimate tensile strength. This can be attributed to the rise in Cr and Mn levels. The addition of Cr enhances the mechanical properties of the weld metal, whereas the incorporation of Mn improves the quality of the weld [39,40,44]. An increase in the Mo percentage was observed to have a positive effect on the formation of acicular ferrite, as well as on the HRD, YS and UTS of the material [39,40]. An increase in Cr content has been observed to directly reduce the formation of acicular ferrite, with the potential for complete elimination at certain levels. A comparison where the Cr ratio is 0.0005 wt.%, reveals a clear correlation between the increasing C and Mn ratio and an enhancement in mechanical properties, including hardness, yield strength, and ultimate tensile strength. While Cr exerts an influence on these mechanical properties, the principal factor responsible for their enhancement is the rising C and Mn ratios [40,44]. An increase in the Cu percentage in the weld metal resulted in a reduction in the formation of acicular ferrite. The addition of Cu resulted in an increase in hardness, yield strength and ultimate tensile strength. These increases can be attributed to the fact that Cu enhances the quality of the weld by facilitating the formation and continuity of the arc. Furthermore, the formation of cracks is reduced as the ductility of the weld metal is increased [50]. The percentages of Ni, C and Mn are provided with parametric variation in data sets. The mechanical properties, hardness, yield strength and ultimate tensile strength including acicular ferrite, increased in direct proportion to the levels of Ni and C [37,41]. The addition of Ni enhanced the ductility and durability of the weld metal, thereby reducing the likelihood of cracking and deformation.

3.3. Acicular ferrite analysis and prediction

Figure 8 illustrates the percentage of acicular ferrite and the corresponding number of data points. The graph illustrates the estimated and predicted values in comparison to the actual and measured values. The percentage of acicular ferrite was estimated for a total of 94 data points, and the mean absolute percentage error (MAPE) between the estimated and actual data was found to be 31.47%. As indicated in Table 3, a MAPE value between 20% and 50% is indicative of an acceptable level of prediction success. Figure 9 demonstrates that the R^2 value is nearly equal to 1 which indicates a successful prediction between the model and the actual data. A notable discrepancy was observed in sample 7 (C: 0.074, Si: 0.33, Mn: 1.45… AF%: 5) in comparison to the predicted value, potentially attributable to the low prevalence of acicular ferrite. However, the AF percentage with 0.074 wt.% C, 1.45 wt.% Mn and 0.33 wt.% Si should give higher ratios of AF around 60% when data in Witt and Witt [33] and Demir [38] are compared on similar compositions. This inconsistency may also be attributed to the MAPE algorithm categorising the predicted value as markedly low in comparison to the trained values within this group during the generation of predicted data by TRAINLM. In general, the LM algorithm is designed to minimise extreme values with the objective of obtaining statistically more realistic results.

The variation of aluminium (Al) and titanium (Ti) percentages shows significant differences, particularly in the range of 0.0006wt% to 0.0255wt% (5% to 76% AF) for Al, and 0.0006wt% to 0.016wt% (72% to 50% AF) for Ti. These fluctuations lead to substantial disparities, as illustrated by the data: 0.0006wt% generates 5% AF, and 0.0016wt% yields 62% AF. Despite the negligible disparity in the values of these percentages, the predicted outcomes appear to exhibit a high degree of reliability.

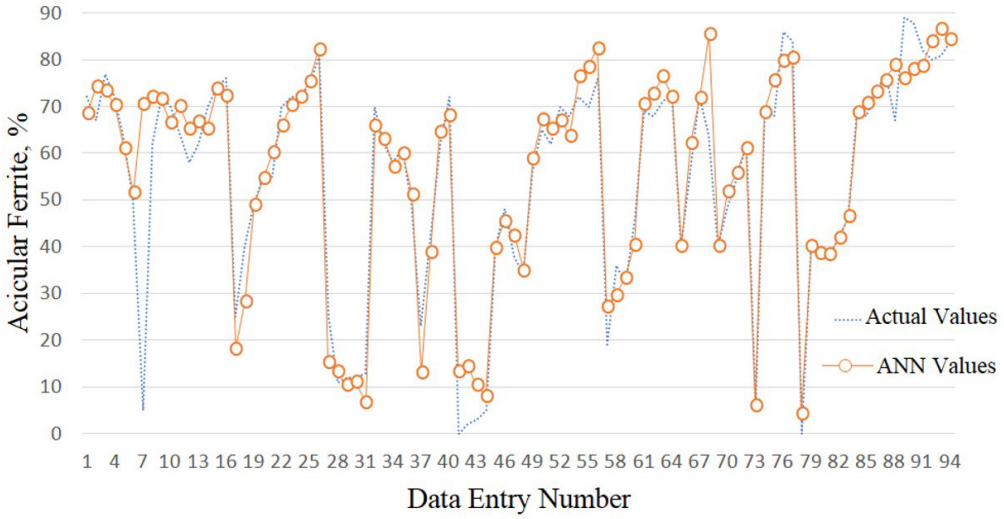

Figure 8. Comparison of actual and predicted Acicular Ferrite percentage values of weld metals studied with respect to data entry number (points).

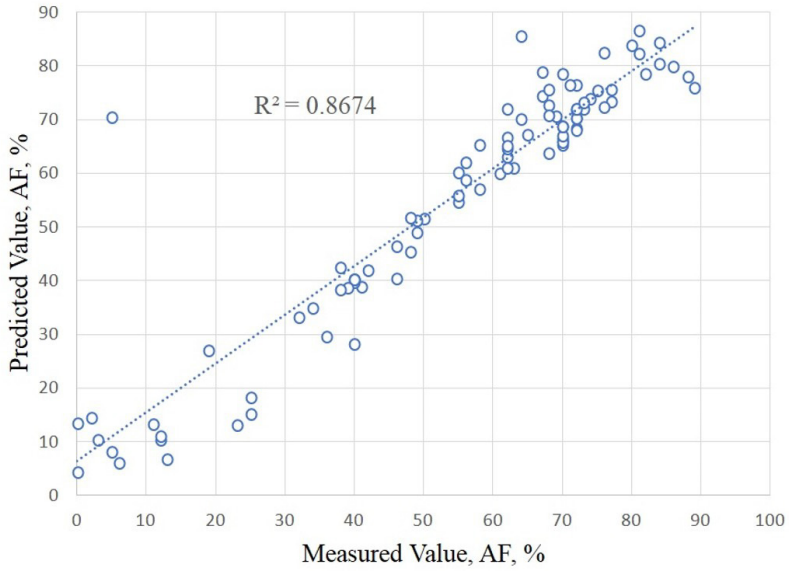

Figure 9. The relationship between the ANN predicted Acicular Ferrite percentages and the measured Acicular Ferrite percentages, displaying R^2 correlation modelling approximation.

3.4. Hardness analysis and prediction

Figure 10 demonstrates the discrepancy between the predicted and actual values of the hardness data obtained from SMAW weld metals. The mean absolute percentage error (MAPE) between the estimated and actual hardness data, derived from a total of 94 data points, is found to be "2.73", which is equivalent to an error value of 2.73%. As previously stated in Table 3, a MAPE value below 10% is indicative of a high degree of prediction success. As illustrated in Figure 11, the R^2 correlation value is also close to 1, which provides further evidence to support the assertion that the predicted value is very accurate. The outliers in HRD prediction output are relatively less compared to AF percentage of ANN predicted values given in Figure 11, which may be a result of instrumental measurement and restricted error margin in the results of hardness.

However, the measured values of hardness demonstrate a minor variation. While the chemical composition is undoubtedly the primary factor influencing hardness, it is the microstructural features within the grain that are of greater significance. It is evident that grains exhibiting higher levels of martensite would yield higher hardness values in comparison to those dominated by AF (Austenite Ferrite) in weld metals. Consequently, the observable discrepancies between the predicted and measured values can be attributed to the unreported microstructural characteristics, such as martensite, polygonal ferrite, bainite, and so forth.

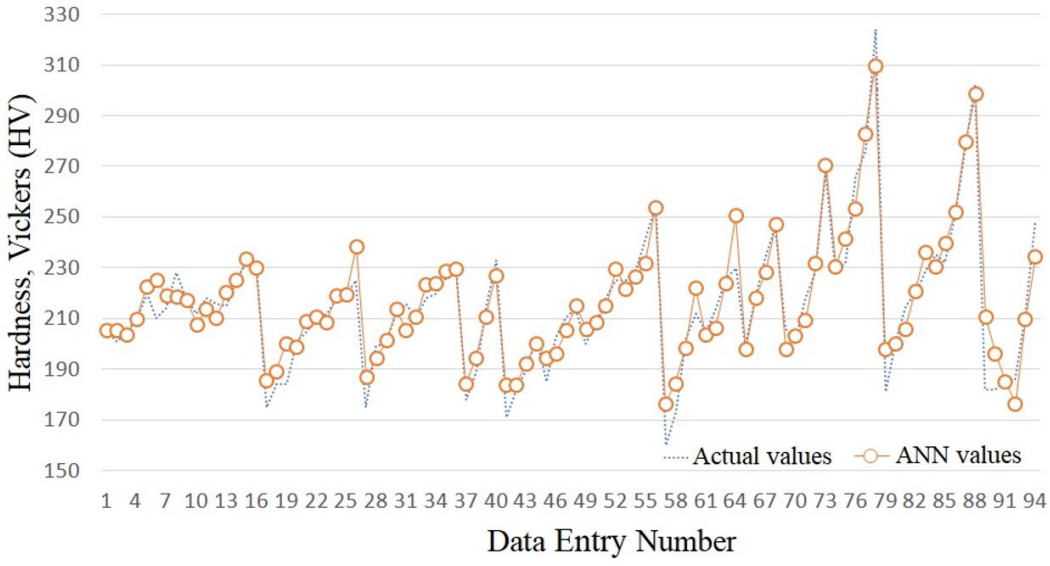

Figure 10. Comparison of actual and predicted Hardness values of weld metals studied with respect to data entry number (points).

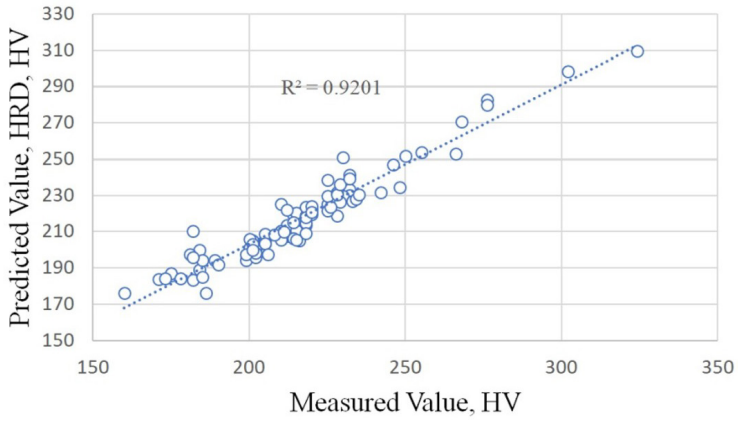

Figure 11. The relationship between the ANN predicted and actual data values, displaying R^2 correlation modelling approximation for the Hardness.

3.5. Yield strength and ultimate tensile strength analysis and predictions

Figure 12 presents a comparison between the predicted and actual values of yield strength of the studied weld metals deposited by SMAW. It appears that predicted values are well within the range and very close approximations have been made successfully. The mean absolute percentage error (MAPE) was calculated to be 2.606% based on 94 data points, indicating a insignificant error rate. As indicated in Table 3, a MAPE value of 10% is indicative of a highly accurate prediction. Furthermore, the R^2 correlation value, which is approximately 0.93, provides additional evidence to support the highly efficient prediction of the model (Figure 13). There are only two outlier values which do not fit in the trendline however these are less likely to largely modify the results of the prediction.

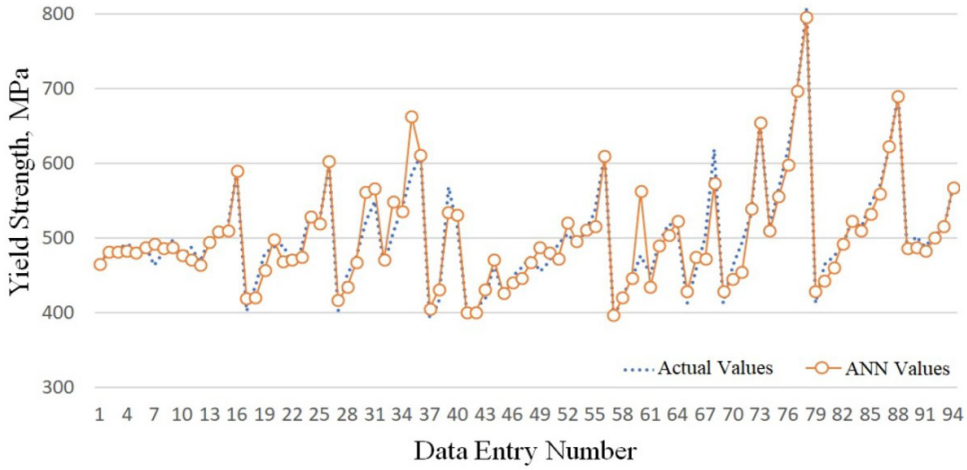

Figure 12. Comparison of actual and predicted YS values of weld metals studied with respect to data entry number (points).

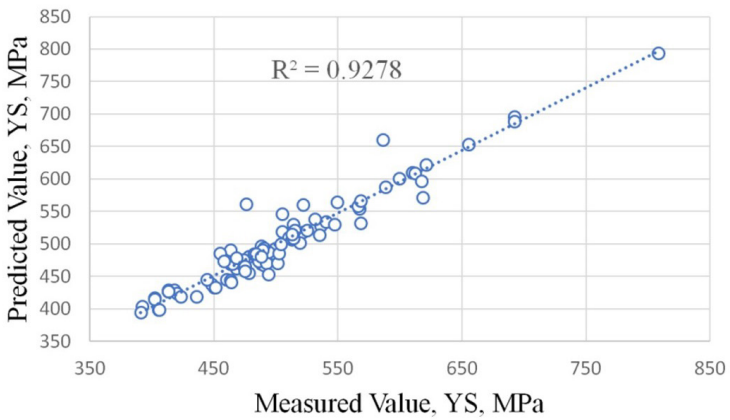

Figure 13. The relationship between the ANN predicted and actual data values, displaying R^2 correlation modelling approximation for the Yield Strength.

Figure 14 illustrates the discrepancy between the estimated/predicted and actual /measured values of ultimate tensile strength. The estimated values are indicated in orange, while the actual values are represented in blue. The ultimate tensile strength was estimated in MPa for 94 data points, and the mean absolute percentage error (MAPE) between the estimated and actual data was found to be "2,347". As previously stated in Table 3, a MAPE value below 10% is indicative of a highly accurate prediction. Figure 15 demonstrates that the R^2 value is nearly equal to 0.89, indicating a comparatively less successful prediction as opposed to YSh values given in Figure 12 and Figure 13. There are two distinct outliers below the trendline and appears to be well below the average values. The lower UTS rate in sample 93 resulted in a notable discrepancy between the predicted and actual values. This discrepancy may be attributed to the TRAINLM algorithm assigning a lower value to the predicted data than to the trained data within this group. UTS values are more affected by the deformation capacity of the steel after YS point where the dislocations become active depending on microstructural features whereas YS is more related to the matrix hardening and atomic distribution in the lattice.

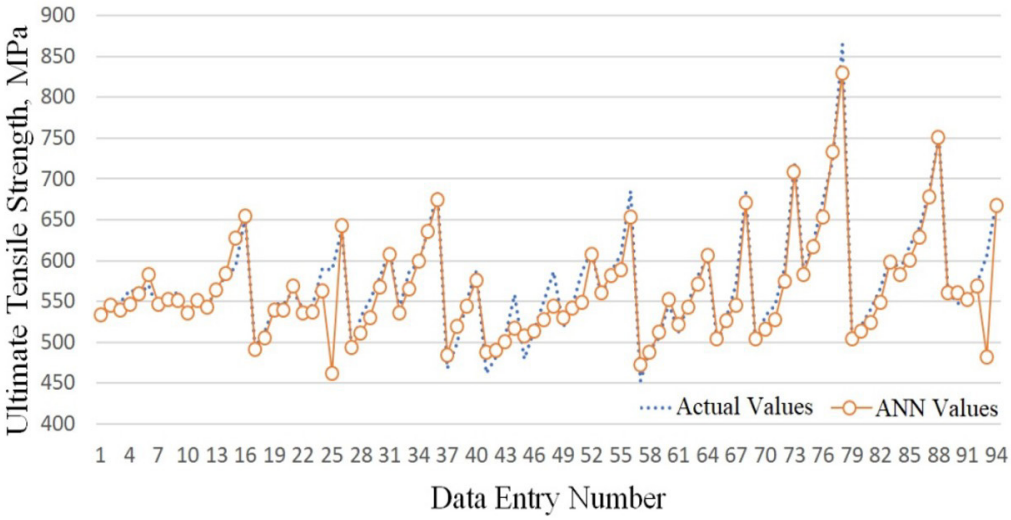

Figure 14. Comparison of actual and predicted Ultimate Tensile Strength values of weld metals studied with respect to data entry number (points).

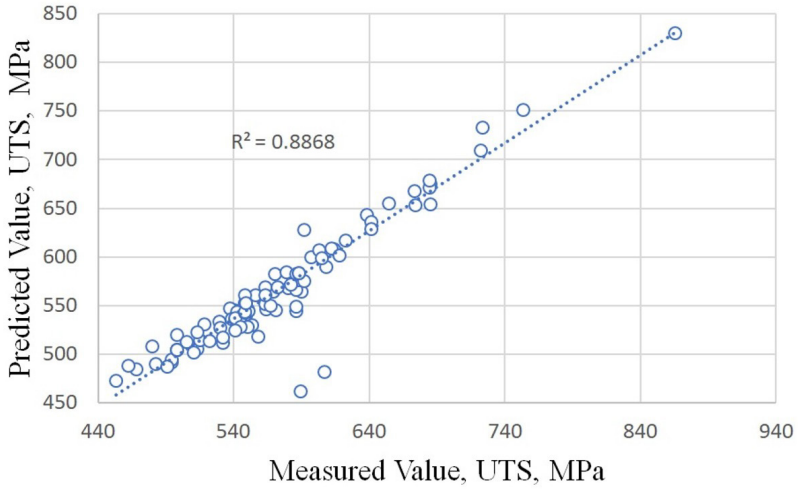

Figure 15. The relationship between predicted and actual data values, displaying R^2 correlation modelling approximation for the Ultimate Tensile Strength.

The chemical and microstructural composition of the weld metal have significant impacts on the overall properties of the welded joint. Accordingly, the relationship between composition and property relationships can yield markedly disparate outcomes when subjected to suitable analytical techniques. For instance, the precision of modelling source properties may be enhanced through the utilisation of diverse techniques, particularly MSE, MAPE, and MAD. The success of the neural network was evaluated using the MAPE, R, and R^2 performance parameters. The R^2 correlation value between the estimated values produced by the neural network and the measured values was calculated as 0.931 for acicular ferrite, 0.959 for hardness, 0.941 for yield strength and 0.963 for ultimate tensile strength. These results demonstrate the efficacy of the interactions in AF, with a success rate of 93.135%, in hardness, with a success rate of 95.923%, in yield strength, with a success rate of 94.17%, and in ultimate tensile strength, with a success rate of 96.324%. The R^2 correlation values were found to be 0.8674,

0.9201, 0.9278 and 0.8868, respectively. The MAPE value for yield strength is within the margin of error of 31.25%. With regard to the measurement of hardness, the MAPE value was found to be within the margin of error of 2.73%. The MAPE value for yield strength is within the margin of error of 2.60%. With regard to ultimate tensile strength, the MAPE value is situated within a margin of error of 2.34%. The MAPE values for hardness, yield strength and ultimate tensile strength are all below 10%. In other words, the neural network demonstrates a high degree of accuracy in predicting these values. In light of these findings, it can be concluded that the predicted values generated by the neural network established in this study are highly reliable and consistent. In this regard, when the percentages of the elements in the weld metal are provided, the acicular ferrite (AF), hardness (HRD), yield strength (YS) and ultimate tensile strength (UTS) can be accurately predicted.

3.6. Prediction of weld metal compositions with respect to training data

As the aforementioned properties, namely hardness (HRD), ultimate tensile stress (UTS), yield stress (YS) and acicular ferrite (AF) percentage, are primarily dependent on the composition of the steel weld, the successful implementation of the model created can ensure the prediction of the weld metal composition of steel welds. The acquisition or prediction of properties with respect to the desired weld metal properties prior to and during the welding of steels will prove beneficial, thus reducing costs, time and labour expenses. Moreover, the capacity to obtain suitable properties will yield commercial benefits in the production of steels whose toughness, hardness, yield strength and ultimate tensile strength can be regulated. In order to obtain a sound prediction of steel weld metal composition, a set of 24 of AF, HRD, UTS and YS values from G.M. Evans' data set [20-29] were used as inputs and processed using the trained artificial neural network. As given in Table 6, this process provided the chemical compositions of the weld metals from which the AF, HRD, YS and UTS values were derived. Then, the prediction results were compared with those of the training set. The outcomes of this analysis indicated that the predictions for certain elements, including Nb, Ni, Cr, Al, and Mn, exhibited an upward bias, while others, such as Mn, demonstrated an underestimation within the dataset. In general, the prediction is poor for the minimum input values such as 0.0005 or 0.0006, these values were difficult to replicate within the series.

Table 6. The following six examples of input, target, output and predicted weld metal compositions (in wt%) are presented, with regard to the selected AF (%), HRD (HV), YS (MPa) and UTS (MPa) values.

	Input			C	Si	Mn	Al	Ti	Nb	V	Mo	Cr	Ni	Cu	N
	AF	5	**T**	0.0740	0.3300	1.4500	0.0005	0.0006	0.0005	0.0005	0.0005	0.0005	0.0005	0.0005	0.0090
1	**HRD**	214	**P**	0.0722	0.3261	0.6842	0.0036	0.0032	0.0249	0.0020	0.0006	0.0054	0.0061	0.0005	0.0069
	YS	463	**R**	0.9757	0.9882	0.4718	7.1602	5.3605	49.876	3.941	1.2539	10.7989	12.203	1.0002	0.7629
	UTS	537	**R^2**	0.9520	0.9765	0.2226	51.268	28.73	2487.58	15.533	1.5723	116.61	148.900	1.0004	0.5820
	Input			**C**	**Si**	**Mn**	**Al**	**Ti**	**Nb**	**V**	**Mo**	**Cr**	**Ni**	**Cu**	**N**
	AF	40	**T**	0.0710	0.3600	0.6300	0.0005	0.0043	0.0005	0.0210	0.0005	0.0005	0.0005	0.0005	0.0078
2	**HRD**	184	**P**	0.0545	0.3226	0.7836	0.0007	0.0027	0.0031	0.0006	0.0007	0.0005	0.0318	0.0005	0.0063
	YS	436	**R**	0.7675	0.8962	1.2438	1.3086	0.6386	6.1221	0.0277	1.3827	1.0222	63.516	1.0060	0.8044
	UTS	513	**R^2**	0.5891	0.8032	1.5470	1.7125	0.4079	37.478	0.0008	1.9118	1.045	4034.31	1.0120	0.6470
	Input			**C**	**Si**	**Mn**	**Al**	**Ti**	**Nb**	**V**	**Mo**	**Cr**	**Ni**	**Cu**	**N**
	AF	77	**T**	0.0760	0.3700	1.3600	0.0190	0.0036	0.0005	0.0005	0.0005	0.0005	0.0005	0.0005	0.0054
3	**HRD**	205	**P**	0.0731	0.3664	1.2060	0.0010	0.0047	0.0016	0.0101	0.0016	0.0005	0.0005	0.0731	0.0084
	YS	485	**R**	0.9621	0.9903	0.8868	0.0519	1.3183	3.1854	20.277	3.1763	1.0063	1.0000	146.10	1.5532
	UTS	549	**R^2**	0.9256	0.9806	0.7864	0.0027	1.7378	10.147	411.16	10.089	1.0126	1.0000	21346.7	2.4123
	Input			**C**	**Si**	**Mn**	**Al**	**Ti**	**Nb**	**V**	**Mo**	**Cr**	**Ni**	**Cu**	**N**
	AF	25	**T**	0.0710	0.3600	0.6300	0.0005	0.0043	0.0005	0.0210	0.0005	0.0005	0.0005	0.0005	0.0078
4	**HRD**	175	**P**	0.0638	0.3157	0.6252	0.0008	0.0048	0.0083	0.0008	0.0011	0.0005	0.0038	0.0005	0.0059
	YS	402	**R**	0.8979	0.8771	0.9925	1.6590	1.1228	16.6131	0.0382	2.1775	1.0004	7.682	1.0053	0.7546
	UTS	494	**R^2**	0.8063	0.7692	0.9850	2.7522	1.2606	275.995	0.0015	4.7413	1.0009	59.011	1.0106	0.5694
	Input			**C**	**Si**	**Mn**	**Al**	**Ti**	**Nb**	**V**	**Mo**	**Cr**	**Ni**	**Cu**	**N**
	AF	86	**T**	0.0370	0.3100	1.0300	0.0005	0.0035	0.0005	0.0005	0.0005	0.0005	0.0005	0.0005	0.0065
5	**HRD**	266	**P**	0.0536	0.3441	0.9760	0.0008	0.0023	0.0032	0.0006	0.0006	0.0005	0.0016	0.0005	0.0069
	YS	617	**R**	1.4474	1.1099	0.9475	1.6303	0.6604	6.3669	1.1235	1.2244	1.0535	3.177	1.0011	1.0571
	UTS	674	**R^2**	2.0949	1.2319	0.8978	2.6578	0.4362	40.537	1.2623	1.4991	1.1099	10.091	1.0022	1.1174
	Input			**C**	**Si**	**Mn**	**Al**	**Ti**	**Nb**	**V**	**Mo**	**Cr**	**Ni**	**Cu**	**N**
	AF	0	**T**	0.0540	0.3300	1.7200	0.0005	0.0035	0.0005	0.0005	0.0005	2.3600	0.0005	0.0005	0.0065
6	**HRD**	324	**P**	0.0535	0.3312	1.7173	0.0007	0.0008	0.0126	0.0062	0.0023	2.3800	0.0124	0.0005	0.0078
	YS	808	**R**	0.9902	1.0035	0.9984	1.3700	0.2153	25.279	12.396	4.5753	1.0085	24.878	1.0165	1.2065
	UTS	865	**R^2**	0.9806	1.0071	0.9969	1.8769	0.0464	639.01	153.66	20.933	1.0170	618.92	1.0334	1.4556

T denotes the target values, P is the predicted values, R is the ratio of the predicted values to the target values, and R^2 is the square root of the predicted values over the target values of the respective elements.

As illustrated in Table 7, the reverse prediction correlation of weld metal compositions with respect to the target weld metal composition is 0.9997. It is crucial to examine the SUMs of weld metal compositions, as the algorithm is highly responsive to the broader range of values, as evidenced by the CORRg column, which represents the elemental correlation between the target and predicted weld metal compositions. It should be noted that the algorithm adjusts the percentages based on its training weld metal composition values, which contain 16 input values for each composition. In order to reach the targeted values of AF, HRD, YS and UTS, some elements that have a greater influence on the input property variations (C, Ni, Cr, O and B, based on the training data and the range of alloying elements in the data set) would need to be increased in order to balance the input and output percentages of elements in the weld metal compositions. The correlation values produced by CORRe were low, yet it is of great significance that CORRs is almost 1. This implies that the correlation coefficient of individual elements is not a reliable indicator, particularly given the narrow range of variation observed in some elements, such as Al, Ti and N. These narrow ranges of variation contribute to the low correlation values observed between the target and predicted weld metal compositions. A further set of data that merits examination in order to evaluate the data set is that of the standard deviations. As shown in Table 7, the standard deviation values for the predicted weld metal compositions are predominantly lower than those for the target weld metal compositions. Evidence suggests that the algorithm is attempting to modify the composition in a manner that leads to average and MAXp values that are generally lower than the target values. In addition, it is suggested that elements with a notable range of property manipulation, such as C and Si undergo corresponding changes. However, the cumulative percentage of elemental composition remains within the specified target range. Consequently, it is viable to sustain this cumulative percentage within the projected value, thus maintaining the limits of the initial composition.

Table 7. The statistical properties of the 24 target (t) and 24 predicted (p) weld metal composition (in wt%) data used in this study.

	STDEVt	STDEVp	AVERAGEt	AVERAGEp	SUMt	SUMp
C	0.0208	0.0137	0.0636	0.0654	5.9799	6.1473
Si	0.1068	0.0581	0.3550	0.3450	33.3700	32.4344
Mn	0.3919	0.3679	1.2313	1.2087	115.7400	113.6147
Al	0.0088	0.0008	0.0023	0.0013	0.2153	0.1189
Ti	0.0032	0.0018	0.0042	0.0033	0.3911	0.3059
Nb	0.0148	0.0070	0.0041	0.0048	0.3836	0.4500
V	0.0168	0.0061	0.0050	0.0051	0.4722	0.4790
Mo	0.1285	0.0013	0.0207	0.0011	1.9455	0.1061
Cr	0.3801	0.3642	0.0901	0.0851	8.4730	7.9975
Ni	0.6158	0.5923	0.1574	0.1526	14.7930	14.3416
Cu	0.1635	0.2151	0.0295	0.0503	2.7740	4.7282
N	0.0014	0.0018	0.0071	0.0064	0.6678	0.6062
	MINt	**MINp**	**MAXt**	**MAXp**	**CORRe**	**CORRs**
C	0.0147	0.0310	0.1480	0.1056	0.3482 (C)	**0.9997**
Si	0.2000	0.2512	0.9500	0.5486	0.4158 (Si)	
Mn	0.6000	0.6005	1.8500	1.8140	0.8770 (Mn)	
Al	0.0005	0.0006	0.0610	0.0050	-0.1058 (Al)	
Ti	0.0006	0.0008	0.0255	0.0110	**-0.0008** (Ti)	
Nb	0.0005	0.0010	0.0940	0.0337	0.3719 (Nb)	
V	0.0003	0.0005	0.1000	0.0337	0.3819 (V)	
Mo	0.0005	0.0005	1.1100	0.0093	0.5334 (Mo)	
Cr	0.0005	0.0005	2.3800	2.3800	0.9549 (Cr)	
Ni	0.0005	0.0005	3.4600	3.4220	**0.9949** (Ni)	
Cu	0.0005	0.0005	1.4000	1.3570	0.8719 (Cu)	
N	0.0010	0.0012	0.0110	0.0093	0.0644 (N)	

The letter p is the abbreviation for the predicted value and t is the abbreviation for the target value. All values except CORRt and CORRp are in wt%; CORRe represents the correlation coefficient of the respective elements and CORRs represents the correlation coefficient of the SUM of the elements of the weld metal compositions in each predicted set.

It is imperative to state that the interaction between the alloying elements can be metallurgically significant when predicting the effect of respective element on certain single property, such as UTS or YS, etc. However, it is important to note that the multiple effects are difficult to analyse, and the cumulative effect of alloying elements is largely irrelevant to each

other. The effect of each element in some of the C-Mn steel weld metal composition of SMAW metals produced by Evans [19-29] was also analysed by Lalam et al. [51-53], who concluded that it is difficult to establish a significant relationship between alloying elements (C, B, O, S, Mo and Nb) and properties such as YS and percentage reduction in cross-sectional area [51-53]. Adopting a different approach on the analysis of the data obtained by Evans [19-29] by Lalam et al [51-53], the cumulative effect of all composition of weld metals is included and a microstructural feature (AF), HRD and UTS are added to the analysis in order to correlate weld metal composition in C-Mn SMAW weld metals. Furthermore, the reverse prediction training of the medel has been tested with some of the input data with a degree of success.

4. Conclusions

Following conclusions can be drawn from this study:

- The neural network demonstrates a high degree of accuracy in predicting values. The success of the neural network was evaluated using the MAPE, R, and R^2 performance parameters. The R^2 correlation value between the estimated values produced by the neural network and the measured values was calculated as 0.931 for acicular ferrite, 0.959 for hardness, 0.941 for yield strength and 0.963 for ultimate tensile strength;
- The success rate of modelling for AF is 93.135%, 95.923% for hardness, 94.17% for yield strength and 96.324% for ultimate tensile strength. The R^2 correlation values were found to be 0.8674, 0.9201, 0.9278 and 0.8868, respectively;
- The MAPE value for yield strength is within the margin of error of 31.25%. With regard to the measurement of hardness, the MAPE value was found to be within the margin of error of 2.73%. The MAPE value for yield strength is within the margin of error of 2.60%;
- With regard to ultimate tensile strength, the MAPE value is situated within a margin of error of 2.34%. The MAPE values for hardness, yield strength and ultimate tensile strength are all below 10%;
- The predictive values generated by the devised neural network are highly reliable and consistent. In this regard, when the percentage ratios of the elements in the weld metal are provided, the AF, hardness, yield strength and ultimate tensile forces can be accurately predicted;
- The weld metal predicted can produce the desired properties prior to and during the welding of steels, thus reducing costs, time and labour expenses and commercial benefits in the production of steels whose toughness, hardness, yield strength and ultimate tensile strength can be controlled;
- Reverse prediction of weld metal compositions revealed that the success rate is relatively high when elements with lowest percentages (usually detection limit or desired levels are very low) are excluded from the calculations. Hence, the algorithm attempts to define a collective composition value in order to adjust to the targeted prediction values of AF, HRD, YS and UTS.

Funding

No funding was obtained for this study.

Authors' contributions

The first draft of the manuscript was written by SD, MS contributed to the calculations and the manuscript review and editing was performed by ST and all authors commented on previous versions of the manuscript. All authors read and approved the final manuscript.

Statements and Declarations

The authors have no competing interests to declare that are relevant to the content of this article. The authors did not receive support from any organization for the submitted work.

References

[1] Islam N, Huang W, Zhuang HL. Machine learning for phase selection in multi-principal element alloys. Computational Materials Science. 2018;150:230-235. http://doi.org/10.1016/j.commatsci.2018.04.003.

[2] Agrawal A, Choudhary A. Deep materials informatics: applications of deep learning in materials science. MRS Communications. 2019;9(3):779-792. http://doi.org/10.1557/mrc.2019.73.

[3] Zhu Z, Liang Y, Zou J. Modeling and composition design of low-alloy steel's mechanical properties based on neural networks and genetic algorithms. Materials. 2020;13(23):5316. http://doi.org/10.3390/ma13235316. PMid:33255378.

[4] Pan H, Peng J, Geng X, Gao M, Miao X. Prediction of mechanical properties for typical pressure vessel steels by small punch test combined with machine learning. International Journal of Pressure Vessels and Piping. 2023;206:105060. http://doi.org/10.1016/j.ijpvp.2023.105060.

[5] Akman T, Yılmaz C, Sönmez Y. Short-term electric energy load forecasting of ankara region using artificial intelligence methods. Journal of Polytechnic. 2023;26(4):1517-1531.

[6] Eren M, Toktaş İ, Özkan MT. Modeling of stress concentration factor using artificial neural networks for a flat tension bar with opposite v-shaped notches. Journal of Polytechnic. 2023;26(3):1199-1205. http://doi.org/10.2339/politeknik.1275466.

[7] Gençer MA, Yumuşak R, Özcan E, Eren T. An artificial neural network model for maintenance planning of metro trains. J Polytechnic. 2021;24(3):811-820.

[8] Toktaş İ, Özkan MT, Erdemir F, Yuksel N. Determination of stress concentration factor (Kt) for a crankshaft under bending loading: an artificial neural networks approach. Journal of Polytechnic. 2020;23(3):813-819. http://doi.org/10.2339/politeknik.683270.

[9] Rumelhart DE, Hinton GE, Williams RJ. Learning representations by back-propagating errors. Nature. 1986;323(6088):533-536. http://doi.org/10.1038/323533a0.

[10] Talaş Ş. The assessment of carbon equivalent formulas in predicting the properties of steel weld metals. Materials & Design. 2010;31(5):2649-2653. http://doi.org/10.1016/j.matdes.2009.11.066.

[11] Padmapriya N, Venkateswaran N, Vijayalakshmi K, Mallieswaran GK, Padmanabhan R. Characterisation of friction stir welds by logistic regression using fractal and wavelet features. Advances in Materials and Processing Technologies. 2019;5(4):582-597. http://doi.org/10.1080/2374068X.2019.1641002.

[12] Genel K. Application of artificial neural network for predicting strain-life fatigue properties of steels on the basis of tensile tests. International Journal of Fatigue. 2004;26(10):1027-1035. http://doi.org/10.1016/j.ijfatigue.2004.03.009.

[13] Acherjee B, Mondal S, Tudu B, Misra D. Application of artificial neural network for predicting weld quality in laser transmission welding of thermoplastics. Applied Soft Computing. 2011;11(2):2548-2555. http://doi.org/10.1016/j.asoc.2010.10.005.

[14] Dhas JER, Dhas SJH. A review on optimization of welding process. Procedia Engineering. 2012;38:544-554. http://doi.org/10.1016/j.proeng.2012.06.068.

[15] Casalino G, Facchini F, Mortello M, Mummolo G. ANN modelling to optimize manufacturing processes: the case of laser welding. IFAC-PapersOnLine. 2016;49(12):378-383. http://doi.org/10.1016/j.ifacol.2016.07.634.

[16] Şık A, Akay A, Bingöl T. Optimization of weld width in submerged arc welding (SAW) method with taguchi method. J ESOGU Eng Arc Fac. 2023;31(1):558-571.

[17] Kurt HI, Oduncuoğlu M, Yılmaz NF, Ergül E, Asmatulu R. A comparative study on the effect of welding parameters of austenitic stainless steels using artificial neural network and Taguchi approaches with ANOVA analysis. Metals. 2018;8(5):326. http://doi.org/10.3390/met8050326.

[18] Thekkuden DT, Mourad AHI. Investigation of feed-forward back propagation ANN using voltage signals for the early prediction of the welding defect. SN Applied Sciences. 2019;1(12):1-17. http://doi.org/10.1007/s42452-019-1660-4.

[19] Evans GM, Bailey N. Metallurgy of basic weld metal. Cambridge: Abingdon Press; 1999.

[20] Evans GM. The influence of Al on the microstructure and properties of C-Mn all weld metal deposits. OERLIKON: Schweibmitt. 1991;49(124):15-31.

[21] Evans GM. The effect of Ti on the microstructure and properties of C-Mn all weld metal deposits. OERLIKON: Schweibmitt. 1991;49(125):22-33.

[22] Evans GM. The effect of V in Mn containing MMA weld deposits. OERLIKON: Schweibmitt. 1991;49(126):18-33.

[23] Evans GM. The effect of Nb in Mn containing MMA weld metal deposits. OERLIKON: Schweibmitt. 1991;49(127):24-39.

[24] Evans GM. The effect of Mo on the microstructure and properties of C-Mn all weld deposits. OERLIKON: Schweibmitt. 1987;45(115):10-27.

[25] Evans GM. The effect of Cr on the microstructure and properties of C-Mn all weld deposits. OERLIKON: Schweibmitt. 1989;47(120):17-34.

[26] Evans GM. The effect of Ni on the microstructure and properties of C-Mn all weld deposits. OERLIKON: Schweibmitt. 1990;48(122):18-35.

[27] Evans GM. Microstructure and mechanical properties of Cu bearing C-Mn weld metal deposits. OERLIKON: Schweibmitt. 1990;48(123):15-31.

[28] Evans GM. The effect of C on the microstructure and properties of C-Mn all weld metal deposits. OERLIKON: Schweibmitt. 1982;40(99):17-31.

[29] Evans GM. The effect of Si on the microstructure and properties of C-Mn all weld metal deposits. OERLIKON: Schweibmitt. 1986;44(110):19-33.

[30] Aggarwal CC. Neural networks and deep learning. Cham: Springer; 2018. http://doi.org/10.1007/978-3-319-94463-0.

[31] Chollet F. Deep learning mit python und keras: das praxis-handbuch vom entwickler der keras-bibliothek. Berlin: MITP Verlags GmbH & Co. KG; 2018.

[32] Nielsen MA. Neural networks and deep learning. San Francisco: Determination Press; 2015. p. 15-24. (vol. 25).

[33] Witt SF, Witt CA. Modeling and forecasting demand in tourism. London: Academic Press; 1992.

[34] Jassim MS, Coşkuner G, Zontul M. Comparative performance analysis of support vector regression and artificial neural network for prediction of municipal solid waste generation. Waste Management & Research. 2022;40(2):195-204. http://doi.org/10.1177/0734242X211008526. PMid:33818220.

[35] Hornik K, Stinchcombe M, White H. Multilayer feedforward networks are universal approximators. Neural Networks. 1989;2(5):359-366. http://doi.org/10.1016/0893-6080(89)90020-8.

[36] Levenberg K. A method for the solution of certain non-linear problems in least squares. Quarterly of Applied Mathematics. 1944;2(2):164-168. http://doi.org/10.1090/qam/10666.

[37] Marquardt DW. An algorithm for least-squares estimation of nonlinear parameters. Journal of the Society for Industrial and Applied Mathematics. 1963;11(2):431-441. http://doi.org/10.1137/0111030.

[38] Demir S. Prediction of mechanical properties of steel based welds with artificial neural networks [Master's thesis]. Afyonkarahisar: Institute of Natural Sciences, Afyon Kocatepe University; 2024.

[39] Gladman T. The physical metallurgy of microalloyed steels. London: Institute of Materials; 1997.

[40] Bhadeshia HKDH. Bainite in steels. 2nd ed. London: IOM Communication Ltd.; 2001.

[41] Lee SG, Lee DH, Sohn SS, Kim WG, Um K-K, Kim K-S, et al. Effects of Ni and Mn addition on critical crack tip opening displacement (CTOD) of weld-simulated heat-affected zones of three high-strength low-alloy (HSLA) steels. Materials Science and Engineering A. 2017;697:55-65. http://doi.org/10.1016/j.msea.2017.04.115.

[42] Keehan E, Karlsson L, Andrén HO, Bhadeshia HKDH. Influence of carbon, manganese and nickel on microstructure and properties of strong steel weld metals: part 3 – Increased strength resulting from carbon additions. Science and Technology of Welding and Joining. 2006;11(1):19-24. http://doi.org/10.1179/174329306X77858.

[43] Gürol U. Welding of high manganese austenitic cast steels using stainless steel covered electrode. International Journal of Metalcasting. 2023;17(2):1021-1033. http://doi.org/10.1007/s40962-022-00834-5.

[44] Cui K, Yang H, Yao S, Li Z, Wang G, Zhao H, et al. Effects of V–N microalloying on microstructure and property in the welding heat affected zone of constructional steel. Metals. 2022;12(3):480. http://doi.org/10.3390/met12030480.

[45] Talaş Ş, Cochrane RC. Effects of Ti on the morphology of high purity iron alloys. Journal of Alloys and Compounds. 2005;396(1):224-227. http://doi.org/10.1016/j.jallcom.2005.01.009.

[46] Takada A, Terasaki H, Komizo Y. Effect of aluminium content on acicular ferrite formation in low carbon steel weld metals. Science and Technology of Welding and Joining. 2013;18(2):91-97. http://doi.org/10.1179/1362171812Y.0000000086.

[47] Zhang C, Gong B, Deng C, Wang D. Computational prediction of mechanical properties of a C-Mn weld metal based on the microstructures and micromechanical properties. Materials Science and Engineering A. 2017;685:310-316. http://doi.org/10.1016/j.msea.2017.01.023.

[48] Chen Y, Zhang D, Liu Y, Li H, Xu D. Effect of dissolution and precipitation of Nb on the formation of acicular ferrite/bainite ferrite in low-carbon HSLA steels. Materials Characterization. 2013;84:232-239. http://doi.org/10.1016/j.matchar.2013.08.005.

[49] Qiao GY, Xiao FR, Zhang XB, Cao YB, Liao B. Effects of contents of Nb and C on hot deformation behaviors of high Nb X80 pipeline steels. Transactions of Nonferrous Metals Society of China. 2009;19(6):1395-1399. http://doi.org/10.1016/S1003-6326(09)60039-X.

[50] Wang JL, Xu N, Wu T, Xi XH, Wang G, Chen LQ. Response of hydrogen diffusion and hydrogen embrittlement to Cu addition in low carbon low alloy steel. Materials Characterization. 2023;195:112478. http://doi.org/10.1016/j.matchar.2022.112478.

[51] Lalam SH, Bhadeshia HKDH, Evans GM, MacKay DJC. Estimation of mechanical properties of C-Mn weld metals. In: IIW Sub-Com; 2000; Sandvik, Sweden. Genoa: International Institute of Welding; 2000. (vol. IIW Doc.II-A-072-00).

[52] Lalam SH, Bhadeshia HKDH, MacKay DJC. Estimation of mechanical properties of ferritic steel welds. Part 1: yield and tensile strength. Science and Technology of Welding and Joining. 2000;5(3):135-147. http://doi.org/10.1179/136217100101538137.

[53] Lalam SH, Bhadeshia HKDH, MacKay DJC. Estimation of mechanical properties of ferritic steel welds. Part 2: elongation and charpy toughness. Science and Technology of Welding and Joining. 2000;5(3):149-160. http://doi.org/10.1179/136217100101538146.